NON-DESTRUCTIVE X-RAY DIFFRACTION INVESTIGATION OF AMPHIBOLE-RICH STONE IMPLEMENTS: WHAT PRECISION SHOULD WE EXPECT FOR GLAUCOPHANE IDENTIFICATION?

AMFIBOL DÚS KŐESZKÖZÖK RONCSOLÁSMENTES RÖNTGEN DIFFRAKCIÓS VIZSGÁLATA: MILYEN PONTOSSÁGRA SZÁMÍTHATUNK A GLAUKOFÁN AZONOSÍTÁSÁBAN?

FERENC KRISTÁLY[1*], ERIKA KERESKÉNYI[2,3]

[1] Institute of Mineralogy and Geology, University of Miskolc, 3515 Miskolc-Egyetemváros, Hungary (*)

[2] Herman Ottó Museum, Mineralogy Department, Kossuth Str. No. 3, 3525 Miskolc

[3] Department of Mineralogy and Geology, University of Debrecen, Egyetem Sqr. 13, 4032 Hungary

E-mail: askkf@uni-miskolc.hu

Abstract

Non-destructive X-ray diffraction has been successfully applied for mineralogical investigation of polished stone implements in several cases. Vertical θ-θ goniometer and parallel beam geometry (with Göbel mirror) are basic instrument requirements for such studies. Rock-forming mineral species can be easily identified, also distinguishing between end-members of compositional series. As a recent development, several members of the amphibole group were successfully identified with this technique. Clear distinction between glaucophane (rock-forming Na-amphibole), actinolite (rock-forming Ca-amphibole) and other amphiboles were tested and successfully confirmed by SEM+EDS analysis.

Kivonat

A csiszolt kőeszközök ásványtani vizsgálatában már többször sikeresen alkalmaztuk a roncsolás-mentes röntgen diffrakciós vizsgálatot. Az eljáráshoz műszeres követelmény a függőleges goniométer és párhuzamos nyaláb geometria (Göbel tükör) megléte. A módszer könnyen alkalmazható a kőzetalkotó ásványok azonosítására, legtöbbször a kémiai összetételbeli sorok végtagjainak azonosítására is. Legújabb eredményeink az amfibol csoport néhány tagjának a megkülönböztetési lehetőségét tárta fel ezzel a módszerrel. Egyértelműen sikerült azonosítani a glaukofánt (kőzetalkotó Na-amfibol), aktinolitot (kőzetalkotó Ca-amfibol) és ezektől különböző amfibolokat,valamint az eredményeket sikeresen alátámasztani SEM+EDS vizsgálatokkal.

KEYWORDS: GLAUCOPHANE, ACTINOLITE, RIETVELD REFINEMENT

KULCSSZAVAK: FITOLIT GLAUKOFÁN, AKTINOLIT, RIETVELD ILLESZTÉS

Introduction

X-ray diffraction (XRD) is one of the most suitable analytical methods to directly identify minerals, observe the presence of non-crystalline components, extract crystal structure related data and calculate absolute quantitative compositions. A pattern recorded on powder samples with an X-ray diffractometer – a diffractogram – contains information in the form of peaks and baseline geometry. For the identification of crystalline components, minerals, the peak properties have to be used: maximum intensity position a.k.a. peak position, maximum intensity value and peak broadening. These are ultimately related to unit cell symmetry and size, chemical composition and crystallite size combined with lattice defects and deformations. In the case of minerals such as amphiboles, where the chemical variability is extremely high, unit cell dimensions are very similar and the crystal lattice may have high defect occurrence, the very precise measurement of peak positions is problematic.

The most widespread type of the X-ray diffraction is powder diffraction (flat powder specimen with smooth surface), requiring grinding and destruction of the investigated materials. Identification of crystalline components is readily done by powerful Search/Match algorithms (database fingerprinting for peak position/intensity sets characteristic for each mineral) and software with high standard graphical user interface. The method can also be used on polished plane surfaces, accounting for preferred orientation (causing anisotropic distortion of peak intensity) and crystallite size effects (causing anisotropic distortion of peak broadening). None the least, powder diffraction is the only way of the technique for precise quantitative analysis and crystal structure determination in mixtures. Conventional powder diffractometers are designed to be used in Bragg-Brentano (parafocusing) geometry, enhancing precision and quality of the

recorded data, but also introducing several errors arising from instrumental set-up and specimen properties. Such errors are sample height precision, flat specimen error and sample transparency error, with a strong impact on measured peak position, peak shape and intensity (for more details see Pecharsky & Zavalij 2005). These errors are produced by the divergent primary beam geometry, and require careful instrument alignment and powder specimen preparation. If the divergent geometry of primary beam can be switched to parallel photon trajectory beam, these errors are eliminated. The solution for switching is the use of parallel beam producing X-ray optics, known as Göbel mirrors (Schuster & Göbel 1995, Deslates et al. 1997) for Bruker AXS Gmbh instruments. The use of Göbel mirror allows for the measurement of not flat or not smooth powder specimens and also block samples with unpolished or even untreated surfaces, the non-destructive application (ND-XRD). A system for sample surface positioning has to be applied (Kristály 2014). On the other hand, some negative features have to be accounted for, like rock texture producing unforeseen preferred orientations, stress and strain leading to unaccounted peak broadening and effect of sample surface on the background of recorded pattern.

In the case of isostructural minerals, like amphiboles, peak broadening has a specific importance. As differences in unit cell dimensions – reflected by the position of peaks –produced by cationic substitutions are very small, a precise instrumental profile model and deconvolution is needed to recognize multiple amphibole species within one sample. Instrumental broadening is higher in parallel beam geometry than Bragg-Brentano (up to 2 times), but empirical profile parametrization on standards allows for the separation of overlapping peaks by deconvolution.

Amphiboles are among several mineral groups which appear in a large specimen variety all with very similar crystal structure and also forming compositional series with several cations substituting each other. Their systematics and detailed grouping is done according to chemical composition (Hawthorne et al. 2012) with the general formula of $AB_2C_5T_8O_{22}W_2$, where A=vacancy, Na, K, Ca, Pb or Li; B=Na, Ca, Mn^{2+}, Fe^{2+}, Mg or Li; C=Mg, Fe^{2+}, Mn^{2+}, Al, Fe^{3+}, Mn^{3+}, Cr^{3+}, Ti^{4+} or Li; T=Si, Al, Ti4+, Be; W=OH^{1-}, F^{1-}, Cl^{1-} or O^{2-}. Precise quantity of these elements is best measured by electron beam microprobe. The most important subgroups for our study are sodium amphiboles and calcium amphiboles, i.e., the groups with the highest rock-forming potential.

The double-chain inosilicate structure of amphiboles crystallizes mostly in two crystal symmetry classes: monoclinic and orthorhombic. Monoclinic amphiboles are known as clino-amphiboles, while orthorhombic varieties are known as orthoamphiboles. According to the difference in unit cell symmetry (given as the space group), distinction between clino- and ortho forms is easily done by XRD, by the distinct position/intensity peak sets characteristic for each series. A more detailed identification of species by XRD is problematic for several reasons. Due to the low symmetry they produce a large number of peaks, most of them located too close to each other (overlapping) for a precise position determination. The amphibole cleavage running along the double chains leads to prismatic-acicular grains even <1 μm, thus strong preferred orientation is general in powder specimen, small intensity peaks may be missing from the pattern. In ND-XRD, the rock texture might produce multiple preferred orientations, leading again to the absence of small intensity peaks. These problems also reduce the applicability of the most important XRD feature for amphibole identification: peak intensity ratios. The differences in chemical composition between distinct amphibole species appear on the XRD pattern as characteristic differences in peak intensity ratios, several times impossible to determine exactly.

In spite of all the limitations and drawbacks, our results show that the identification of several amphibole species is possible even by ND-XRD, if all the instrumental and measurement effects are accounted for.

Materials and methods

Polished stone implements of amphibole-rich compositions were identified in the archaeological collection of the Herman Ottó Museum (Miskolc, Hungary). These implements have been previously studied for petrography and mineralogy by Józsa et al. (2001a, 2001b), but our results provide the first detailed mineralogical composition. Macroscopic features of the selected implements suggested mesometamorphic rocks, the green and black dominant colors referring to actinolite and similar amphiboles. A more detailed petrographic study (Kereskényi et al. 2016)revealed similarities with blueschists from the area of Hačava (Meliata Unit, Slovakia). Macroscopically the axes are fine-grained, having bluish, bluish green, greenish, greyish blue colour. Some of them are strongly foliated, but most of them are massive, non-foliated (Kereskényi et al. 2016). The blueschist sample 89.9.11. has amphiboles as cc. 1-mm-sized enhanced contoured, green, rounded patches in the dark matrix. The dimensions of the flat-chisel are the following: length 3 cm, width 2.5 cm, thickness 0.5 cm. In the blueschist sample the contours of the green amphibole spots are blurred and elongated in the direction of foliation. The dimensions of the flat-axe: length 6 cm, width 5.4 cm, thickness 1.2 cm. Results of a nephrite implement from an earlier

work (Péterdi et al. 2014) was used for comparison by the permission of Katalin T. Biró (Hungarian National Museum, Budapest). The surfaces selected for mineralogical analysis by XRD were cleaned with acetone.

Measurements were carried out on a Bruker D8 Advance diffractometer (Cu-Kα source, 40 kV and 40 mA generator settings) with a vertical θ-θ goniometer (radius 250 mm) and a Vantec1 positions sensitive detector (PSD). The parallel beam geometry was obtained with a W-C multilayer Göbel mirror (2nd generation, 2005) operated with a 0.6 mm beam exit slit and 2.5° axial Soller slit. The PSD detector was also equipped with a 2.5° axial Soller slit, while antiscattering and detector slits were switched according to the detector window opening degree. Most of the measurements were run with 5° detector window opening. Patterns were recorded from 2 °(2θ) to 90 or 100 °(2θ) with 0.007 °(2θ) step per 24 seconds. For sample surface positioning a microscope stative with micrometric screw was used, aligning the surface to the beam was done by using an Al foil stripe on the surface selected to be measured (Kristály 2014). The measurement was run with the Al foil attached to the surface, for the possibility of using Al peaks if peak position corrections are required. The Al foil reduced diffracted intensity by 1% in number of counts as compared to measurements without the foil. The illuminated sample are on a flat specimen is 12x8 mm at 30 °(2θ), but varies highly depending on the curvature of the surface.

Peak broadening and profile were determined on NIST 1976b corundum plate, while empirical profile parametrization was done on NIST SRM640d silicon powder. The diffractometer has a 0.05 °(2θ) broadening in terms of FWHM at 30 °(2θ) in Bragg-Brentano geometry with symmetrical 2.5° axial-Sollers, divergence and antiscattering slits 0.6 mm, detector slit 0.2 mm. With Göbel mirror and Vantec1 PSD this broadening was modified to 0.140 °(2θ) at 30 °(2θ) keeping symmetrical 2.5° axial-Sollers, 0.6 mm exit slit, 8 mm antiscattering and 12 mm detector slit. No significant peak asymmetry was observed for $K\alpha_1$ wavelength. These parameters have negative impact on peak overlapping delimitation, thus more than usual experience is required at evaluation.

Results were subjected to data reduction by Fourier polynomial noise filtering and baseline fitting with a 3rd degree gliding polynomial. Search/Match analysis was run in Bruker Diffrac*Plus* EVA on the ICDD (International Centre for Diffraction Data) PDF2 (Powder Diffraction Files) 2015 and COD (Crystallography Open Database) (Grazulis et al. 2009) databases. Whole powder pattern decomposition, Rietveld refinement (Young 1993) and comparative crystal structure based simulations were run in TOPAS4 software, using ICSD (Inorganic Crystal Structure Database) and AMCSD (American Mineralogist Crystal Structure Database) crystal structure data. Glaucophane data was adjusted also according to Comodi et al. (1991).

SEM+EDS measurements were carried out on a Jeol JXA 8600 Superprobe with 20 kV accelerating voltage and 20 nA probe current, on carbon coated surfaces, according to the method described by Bendő et al. (2013) for non-destructive investigation.

Results and discussion

Simple mineralogy

On a flat, well-polished implement surface (nephrite, **Fig.1.**) good quality pattern can be obtained with measurement as short as 1 minute, with noise as the only difference to the pattern measured on the same surface within 15 minutes (**Fig. 2.**).

The investigated implement was a nephrite tool, and the first match on the Search/Match list was actinolite (**Fig. 2**.), fully in accordance with the rock being nephrite. The chemical compositions given in the ICDD PDF and COD databases are orientative and cannot be considered as corresponding to the investigated material. However, good quality cards will show an approximately good chemical composition, comparable to microprobe data (although in PDF 89-5366 the elements are not listed according to actual amphibole nomenclature, and we disregard F content). Details on SEM+EDS chemical analysis of this implement can be found in Péterdi et al. (2014).

Fig. 1.: Nephrite chisel from private collection of Gy. Kerékgyártó (15 x 2 cm)

1. ábra: nefrit véső Kerékgyártó Gy. magán-gyűjteményéből (15 x 2 cm)

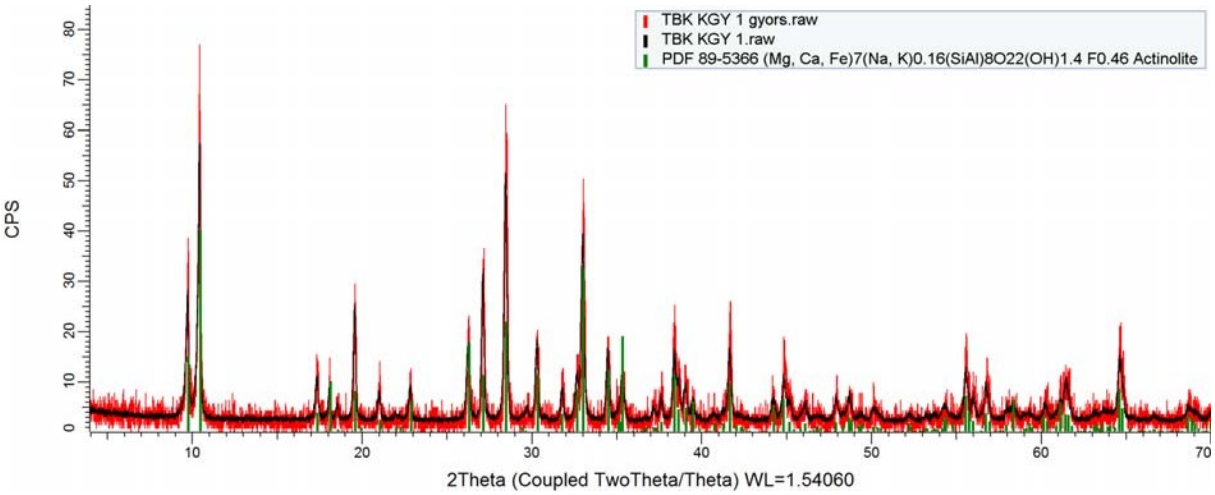

Fig. 2.: XRD patterns taken on the flat surface of the nephrite implement. Red pattern measured in 1 minute, black pattern measured in 15 minutes (original curves).

2. ábra: A nefrit eszköz lapos felületén felvett XRD görbék. Pirossal az 1 perces mérés, feketével a 15 perces mérés eredménye (eredeti felvett görbék).

Lightly complicated mineralogy

On implements with undulated or convex surfaces (in this case, blueschist, sample 89.9.11, **Fig. 3.**) the baseline of the pattern becomes more complex (**Fig 4.**), especially in the <6 °(2θ) range due to the "shadowing" effect of the measured surface.

As a consequence, background subtraction requires more attention, but the identification of peaks is still possible, as shown on chloritic implements in Kristály (2014). The first hit on the Search/Match list with routine settings is ferroglaucophane, also encountering the worst problem of database entries: multiple cards with different data (**Fig 3.**).

Also, a large number of other amphiboles and unrelated minerals appear on the list, requiring a deeper inspection of the Search/Match list. The identification of minor to accessory components requires more steps and "tricks", thus it is not presented here.

Comparing Search/Match results with SEM+EDS data, the glaucophane composition was found to be dominant (**Fig 4., Table 1.**), with significant epidote and titanite, and minor clinochlore. Albite grains also appear, in concordance with XRD results.

The chemical compositions measured in several points show a very similar *a.p.f.u.* (atoms per formula unit) distribution, as given in the selected PDF card at Search/Match, except for the Fe- and Mg-content.

Fig. 3.: blueschist implement from the collection of the HOM, Inv. nr. 89.9.11.

3. ábra: kékpala csiszolt véső töredéke a Herman Ottó Múzeum gyűjteményéből, ltsz. 89.9.11.

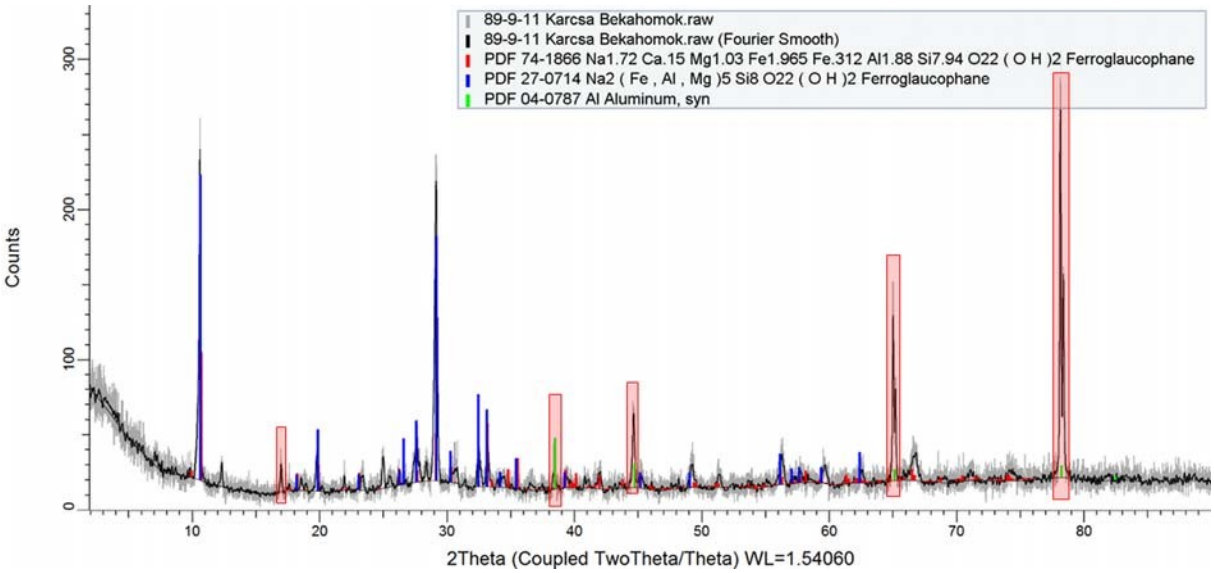

Fig. 4.: XRD pattern recorded (15 minutes) on the blueschist implement 89.9.11, grey is the original, black is the noise reduced pattern, red rectangles mark the Al peaks (except for the peak at 17 °2θ, which appears on this foil, also checked separately, but crystallographic relation to the Al structure was not found).

4. ábra: A kékpala baltán (89.9.11 leltári szám) felvett görbe (15 perces mérés), szürke az eredeti, fekete a simított görbe, piros téglalapok az Al csúcsait jelölik (kivéve a 17 °2θ-nál lévő csúcsot, amely ennél a fóliánál megjelenik, külön ellenőrizve is, de az Al szerkezettel való kristálytani kapcsolatát nem találtuk meg).

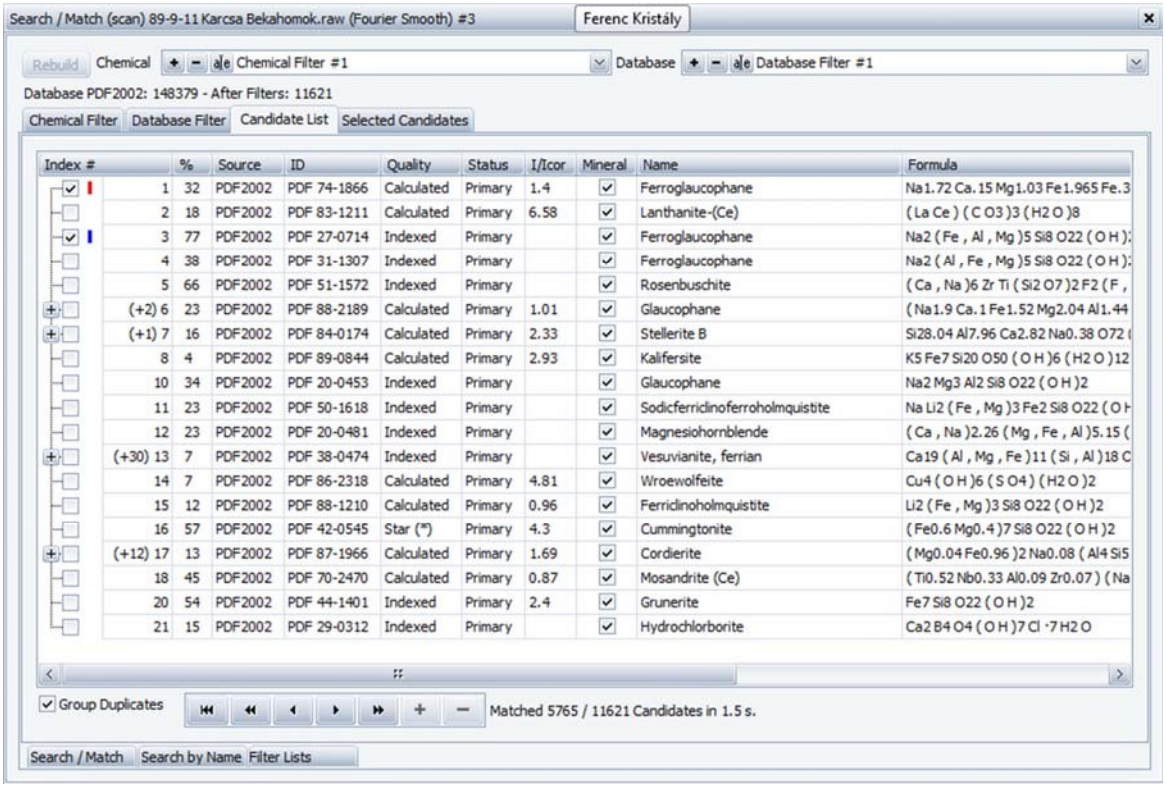

Fig 5.: Search/Match results panel in the first evaluation step, on the noise reduced and background fitted pattern in Fig 2.

5. ábra: A kiértékelés első lépésének Search/Match eredményi ablaka, a simított és háttérillesztett görbén a 2. ábráról

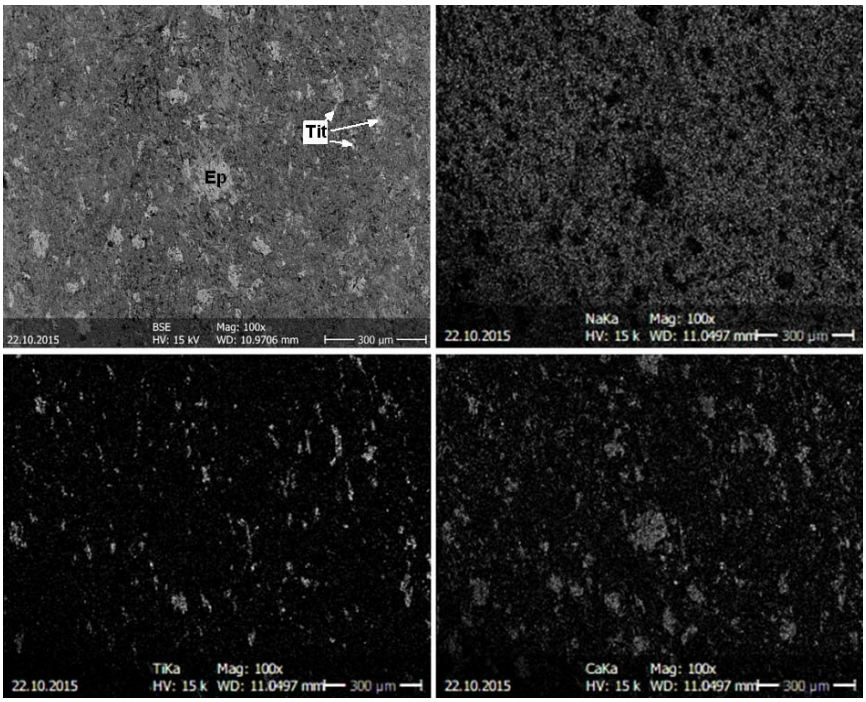

Fig 6.: BSE image (top-left) and X-ray maps of the 89.9.11 blueschist implement, Na is mainly glaucophane (albite not distinguished), Ti is only titanite, Ca is epidote and titanite.

6. ábra: BSE kép és elemtérképek a kékpala baltára (89.9.11 leltári szám), a Na főleg glaukofánt (az albit nem megkülönböztethető), a Ti csak titanitot, a Ca epidotot és titanitot jelöl.

Table 1.: SEM+EDS results of the investigated implements, representative results only (XRD data taken from PDF 74-1866 file)

1. táblázat: SEM+EDS mérési eredmények a vizsgált mintákon, csak a legjellemzőbb eredmények (XRD-re vonatkozó adatok a PDF 74-1866 kártyáról)

		Na	K	Ca	Mg	Fe^{2+}	Fe^{3+}	Al	Si	Ti
	theo. gl	2	0	0	3			2	8	0
	theo. fgl	2	0	0		3		2	8	0
89.9.11	XRD	1.72	0	0.15	1.03	1.97	0.31	1.88	7.94	
	1	1.83	0.01	0.02	1.96	1.09		2.04	7.98	0
	2	1.90	0.01	0.11	2.11	1.18		1.83	7.95	0
	3	1.82	0.01	0.06	1.94	1.16		2	7.97	0
	4	1.93	0.01	0.08	1.85	1.40		1.83	7.97	0.01
B14	XRD	1.72	0	0	1.03	1.97	0.31	1.88	7.94	0
	1*	0.16	0	1.84	3.77	0.62	0.26	1.22	7.21	0
	2	1.21	0	0.84	2.57	1.63	0	0.91	7.97	0
	3	1.97	0	0.16	2.29	1.41	0	1.40	8.01	0
	4	2.01	0	0.13	1.81	1.89	0	1.28	8.10	0

*results indicating composition closed to winchite

The reason behind the observation is that Fe^{2+} and Mg replacing each other produce only minor change in peak XRD positions, due to the similar cation size. As a consequence, the ND-XRD results may indicate ferroglaucophane, because we cannot correct for the texture and stress-strain peak position distortions of the rock sample.

To observe the degree of sample related distortions, we can try to solve the XRD pattern by Rietveld refinement, simulating a pattern for each mineral, and creating a scaled sum pattern, which is compared to the measured data. In this case, an acceptable solution (**Fig 7.**) was found after applying preferred orientation PO and stress-strain corrections to the identified minerals.

Calculated unit cell data of glaucophane is given in **Table 2.**, displaying minimal differences from theoretical data (Fehér 2009, also on http://handbookofmineralogy.org/).

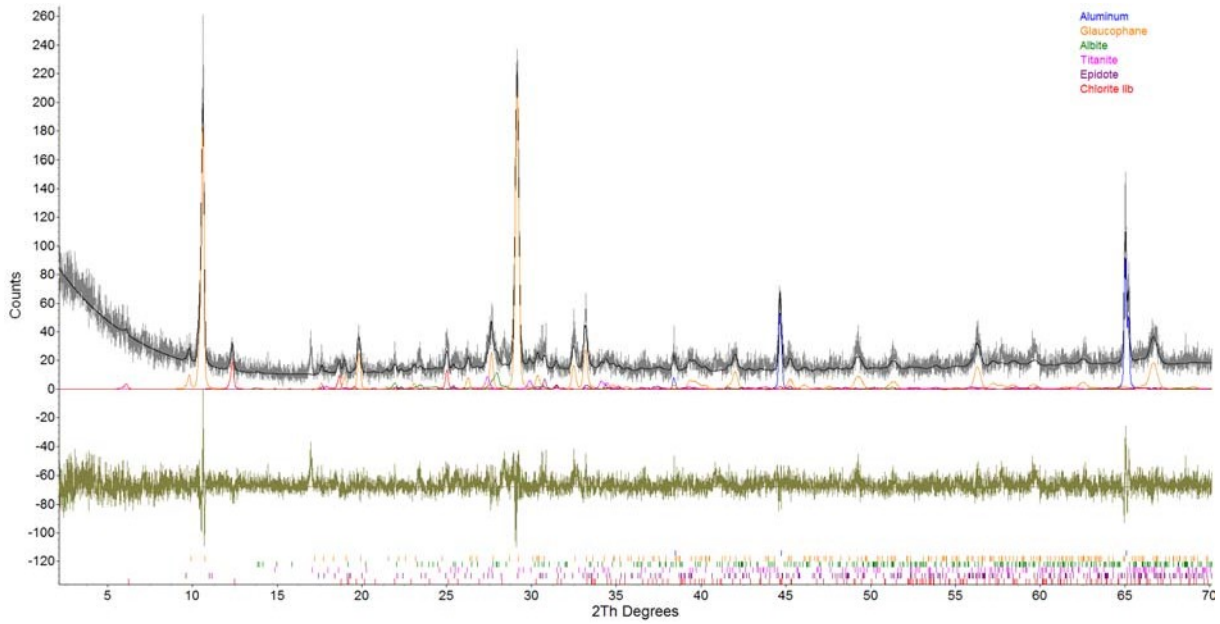

Fig 7.: Rietveld refinement patterns of the investigated blueschist implement, sample 89.9.11 (gray – measured, black – calculated, olive – difference, and each single pattern for the minerals with the given color)

7. ábra: A Rietveld illesztés eredménye a vizsgált, 89.9.11 leltári számú kékpala eszközön (szürke – mért, fekete – számolt, zöld – különbség, illetve minden ásványnak az adott színnel jelölt önálló görbéje)

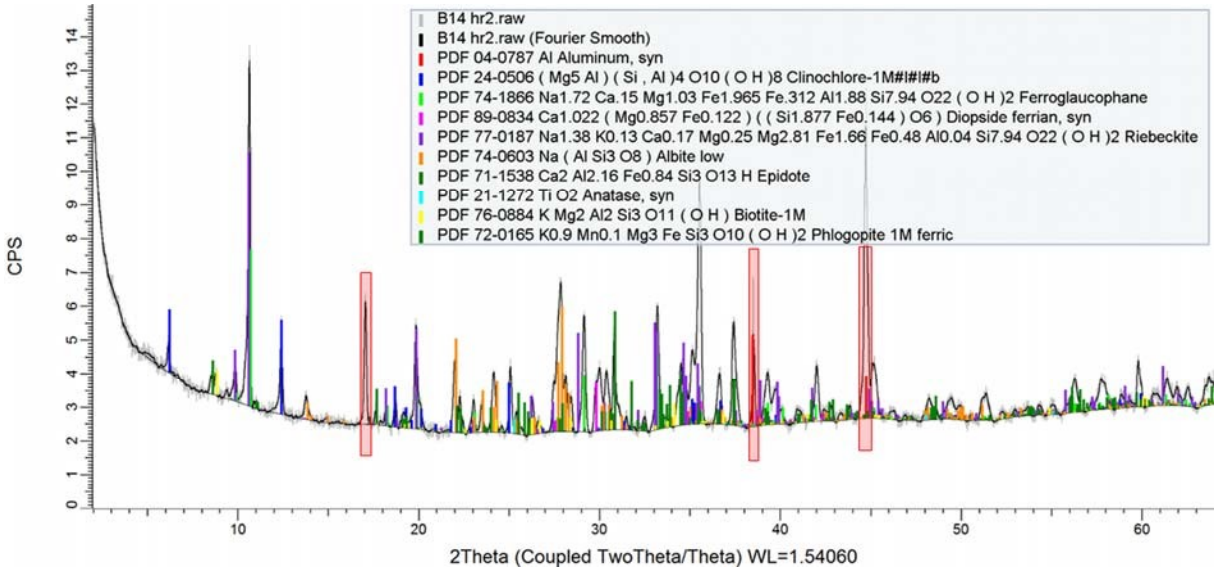

Fig 8.: XRD pattern recorded (15 minutes) on the blueschist implement B14, grey is the original, black is the noise reduced pattern, red rectangles mark the Al peaks(except for the peak at 17 °2θ, which appears on this foil, also checked separately, but crystallographic relation to the Al structure was not found).

8. ábra: A B14 mintaszámú kékpala baltán (Felsővadász-Várdomb, leltározatlan anyag a HOM gyűjteményében) felvett görbe (15 perces mérés), szürke az eredeti, fekete a simított görbe, piros téglalapok az Al csúcsait jelölik (kivéve a 17 °2θ-nál lévő csúcsot, amely ennél a fóliánál megjelenik, külön ellenőrizve is, de az Al szerkezettel való kristálytani kapcsolatát nem találtuk meg).

Fig. 9.: blueschist implement from the collection of the HOM, Ref. Nr. B14, Felsővadász-Várdomb

9. ábra: B14 sz. kékpala csiszolt véső töredéke a Herman Ottó Múzeum gyűjteményéből, Felsővadász-Várdomb

Complicated mineralogy

For an implement (in this case, blueschist, sample B14 (**Fig. 9.**)) with more than three rock-forming minerals, the quality of the measured surface is even more significant. As observed on the darker, streaked blueschist implements, the low angle background might also lead to false peak determinations (**Fig. 9.**), which can be eliminated by repeated measurements for finding a good surface.

The Search/Match returned riebeckite as possible 2nd amphibole after ferroglaucophane (both glaucophane and ferroglaucophane are members of the Na amphibole group), and also several minor rock-forming minerals. Depending on personal decision making of the Search/Match results sorting, winchite (a Na-Ca amphibole) can also be nominated as matching. Such case is frequent even in powder diffraction of samples with similar minerals. However, taking a look at the structural differences of the three species, the chances for a perfect identification without chemical analysis are minimal.

SEM+EDS results show glaucophane > ferroglaucophane > winchite as major minerals, associated with augite, omphacite, albite, epidote, clinozoisite and phlogopite, clinochlore and titanite as minor components (**Fig. 10.**).

Rietveld refinement and related corrections (**Fig. 11.**) almost gave the same result as SEM+EDS, except for winchite, where the XRD pattern was too complicated to obtain conclusive deconvolution. Calculated unit cell parameters for glaucophane and ferroglaucophane are listed in **Table 2**.

Riebeckite, as a suggested match for the XRD pattern was omitted, since it was not necessary to obtain amphibole peaks solution in fitting and it was missing from the SEM-EDS results, too. Refinement with winchite returned too low contribution, meaning that resolving glaucophane and riebeckite or winchite requires higher instrumental precision and selection of surfaces with more contribution of these species.

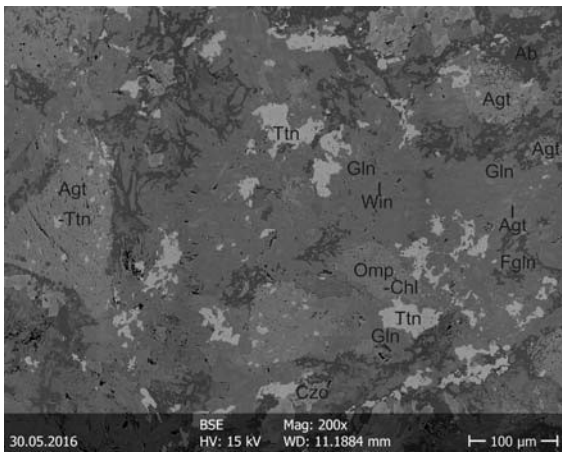

Fig. 10.: BSE image of the B14 blueschist implement, Agt=augite, Czo=clinozoisite, Fgln=ferroglaucophane, Gln=glaucophane, Omp=omphacite, Ttn=titanite, Win=winchite.

10. ábra: BSE kép a B14-es mintaszámú kékpala baltára, Agt=augit, Czo=klinozoisit, Fgln=ferroglaukofán, Gln=glaukofán, Omp=omfacit, Ttn=titanit, Win=winchite.

Table 2.: Calculated unit cell parameters

2. táblázat: Számolt elemi cella paraméterek

	theo. gl	89-9-11	B-14 gl	B-14 fgl	theo fgl
a (Å)	9.595	9.561 ± 0.01	9.567 ± 0.02	9.585 ± 0.01	9.587
b (Å)	17.798	17.806 ± 0.04	17.806 ± 0.03	17.797 ± 0.04	17.832
c (Å)	5.307	5.289 ± 0.03	5.306 ± 0.04	5.322 ± 0.01	5.315
beta (°)	103.66	103.49 ± 0.03	103.71 ± 0.12	103.66 ± 0.02	103.47

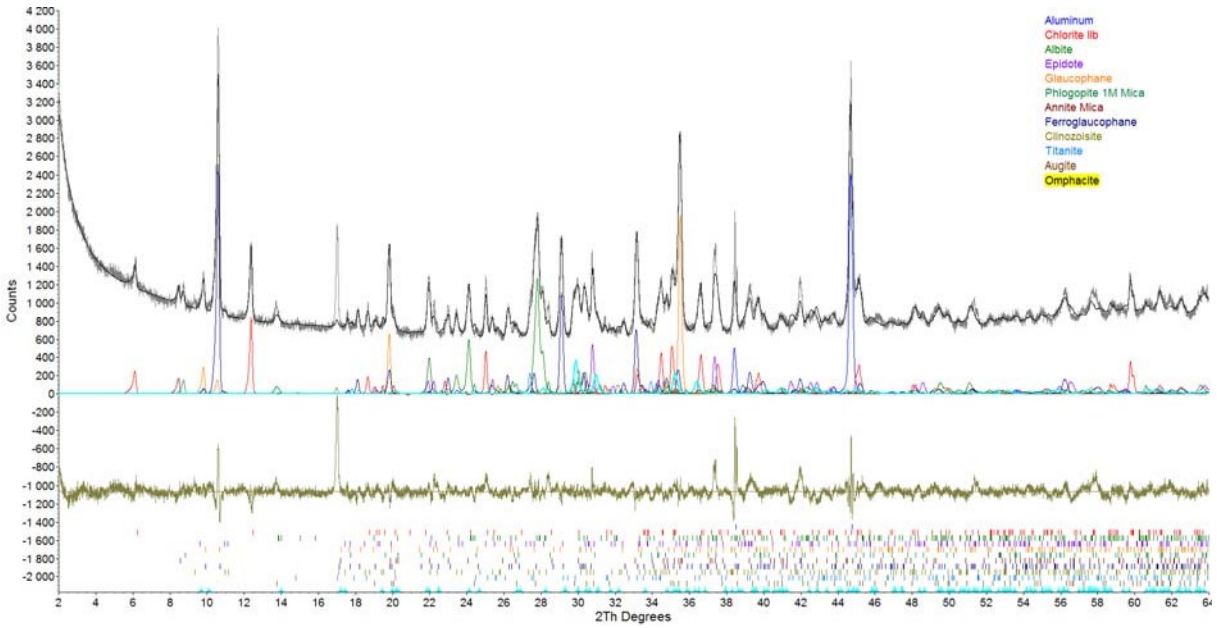

Fig. 11.: Rietveld refinement patterns of the investigated blueschist implement, sample B14 (gray – measured, black – calculated, olive – difference, and each single pattern for the minerals with the given color)

11. ábra: A Rietveld illesztés eredménye a vizsgált, B14 számú kékpala eszközön (szürke – mért, fekete – számolt, zöld – különbség, illetve minden ásványnak az adott színnel jelölt önálló görbéje)

Comparison of amphibole calculated patterns

To understand the basis of amphibole species identification, it is useful to observe the differences on calculated (simulated) XRD patterns. In TOPAS4, we have the possibility to simulate also instrumental contributions, crystallite size effects and stress-strain distortions. In **Fig. 12a** we have a direct comparison of several end-member amphiboles, calculated with theoretical unit cell dimensions and cell content. We have omitted background contribution from the simulations. In the first step, we considered the actual settings and configuration of the instrument and calculated patterns for un-oriented specimens of 1 μm crystallite size.

he resulting patterns show that these species can be differentiated in the case of a well-aligned diffractometer and correctly adjusted sample. Also we have to note that only the 8-12 °2θ region (for Cu-Kα, covering 11-7.3 in Å) is useful, especially if feldspars and other low symmetry rock forming minerals are present (**Fig. 12b**). However, considering 1 μm crystallite size for metamorphic amphiboles is idealistic, due to the many crystal lattice defects and deformations. Thus, in a next step we simulated patterns for 0.1 μm crystallite size, observing a huge drop in expected intensity and also broadening which leads to problems in peak overlapping recognition (**Fig. 12c**). In the 3rd step we have simulated another highly possible situation in metamorphic rocks, the high stress-strain related deformation. Applying E_0=0.75 stress, we obtain even larger broadening and intensity reduction (**Fig. 12d**), yet it is possible to decide whether the glaucophane-like (Na-amphibole) or the actinolite-like (Ca-amphibole) amphibole is dominant. Combining 0.1 μm crystallite size and E_0=0.75 stress, we arrive to the extreme case, where amphibole distinction is expected to be uncertain (**Fig. 12e**).

Besides peak positions, intensity ratios of the two peaks (*020*) and (*110*) are indicative for group level categorization – if we keep in mind the texture and effect of measured surface geometry. With increasing Fe^{2+} content the intensity of (*110*) peak (~ 10.5 °2θ on **Fig. 12**) is multiply increased as compared to (*020*)(~ 9.55 °2θ on **Fig. 12.**). The peak position differences are related to cation size differences, these two peaks representing crystallographic directions over which octahedral size and conformation has the main impact on interplanar distances.

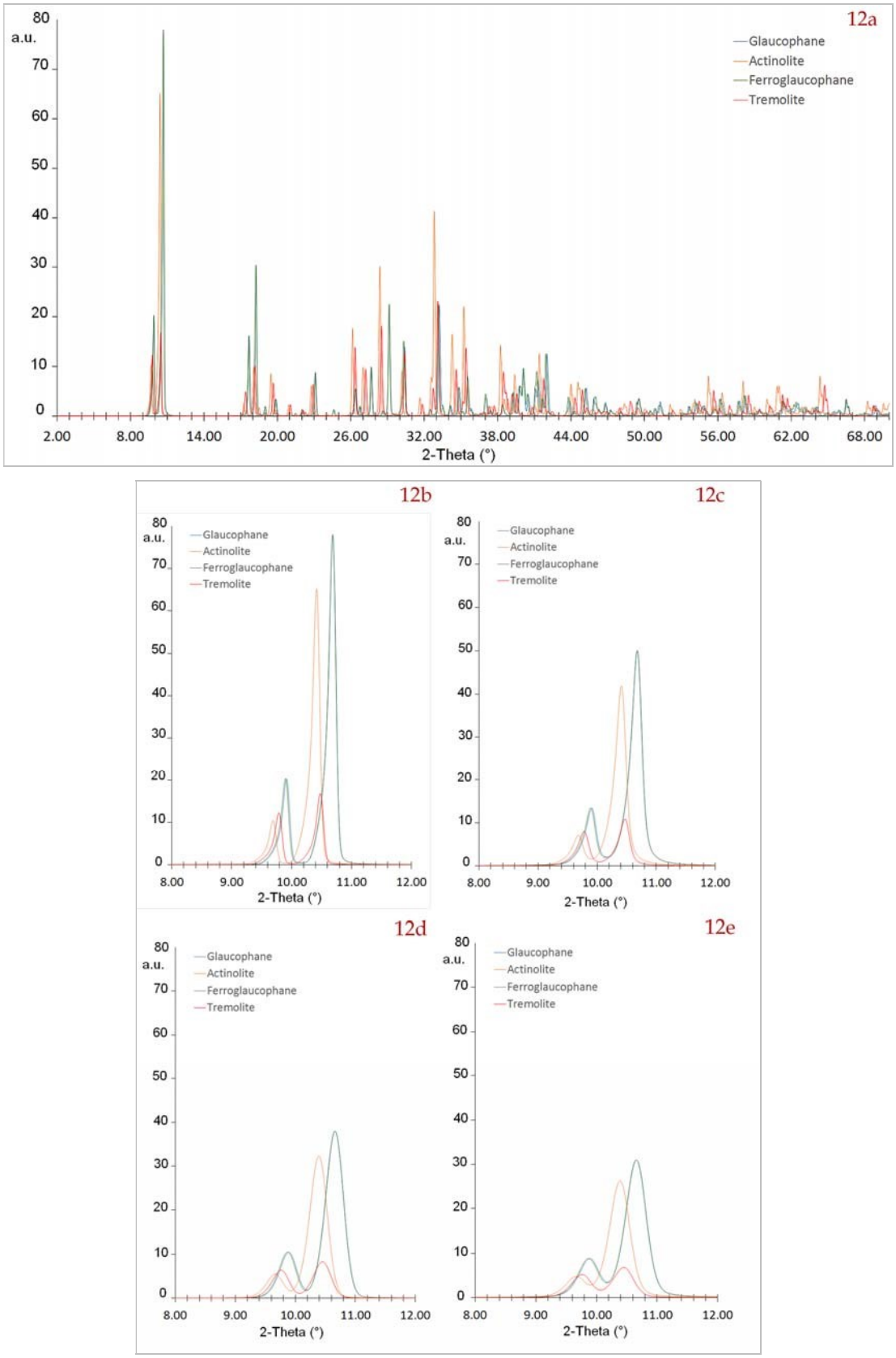

Fig. 12.: Simulated patterns for several amphibole species. a: large angular range, b: zoomed in section of 9a, c: crystallite size broadening simulation, d: stress-strain broadening simulation, e: crystallite size and stress-strain coupled simulation.

12. ábra: Számolt görbék néhány amfibol fajra. a: széles szögtartomány, b: a 9.a kép kivágott részlete, c: krisztallit méret kiszélesedés szimulációja, d: feszültség kiszélesedés szimulációja, e: krisztallit méret és feszültség okozta kiszélesedés szimulációja

Conclusions

According to our measurements, calculations and comparative data evaluation, we suggest that the differentiation between actinolite, tremolite (both Ca-amphiboles, with varying iron content) and glaucophane (a rock-forming member of the Na-amphibole group) is reliable from ND-XRD, if the instrument has a well aligned goniometer (0-point error < 0.01 °2θ), the sample centering can be accurately verified and a well-established Search/Match evaluation procedure can be combined with deconvolution and Rietveld-refinement based (or similar) whole powder pattern fitting. Correct modelling of instrumental profile is a mandatory condition.

SEM-EDX analyses of the similar surfaces provide useful complementary chemical data, helping to better differentiate in the Na-amphibole group (glaucophane vs. ferroglaucophane).

These non-destructive methods provide basic information on the composition of archaeological implements with great value or unique features.

Acknowledgements

This work was carried out as part of the TÁMOP-4.2.2.A-11/1/KONV -2012-0005 project, under the auspices of the Center of Excellence of Sustainable Resource Management, in the framework of the New Széchenyi Plan. The authors are thankful to Dr. Katalin T. Biró for the permission on using XRD data and providing photograph of the nephrite implement. The authors are grateful to Dr. Erzsébet Harman-Tóth and Dr. Bálint Péterdi for the useful comments and corrections in improving the manuscript.

References

BENDŐ Zs., OLÁH I., PÉTERDI B., SZAKMÁNY Gy., HORVÁTH E. (2013): Non-destructive SEM-EDX analytical method for polished stone tools and gems: opportunities and limitations. *Archeometriai Műhely* **2013 (X/1)**, 51–66.

COMODI P., MELLINI M., UNGARETTI L., ZANAZZI P. F. (1991): Compressibility and high pressure structure refinement of tremolite, pargasite and glaucophane. *European Journal of Mineralogy* **3** 485–499

DESLATES, R.D., STAUDENMANN, J.L, HUDSON, L.T., HEINS, A. & CLINE, J.P. (1997): Parallel beam powder diffractometry using a laboratory X-Ray source. *International Centre for Diffraction Data, Advances in X-ray Analysis* **40** 225–236.

FEHÉR B. (2009): *Ásványkalauz*. Magyar Minerofil Társaság, Miskolc, 624 p.

GRAŽULIS S., CHATEIGNER D., DOWNS R.T., YOKOCHI A.F.T., QUIRÓS M., LUTTEROTTI L., MANAKOVA E. BUTKUS J., MOECKG P. & LE BAIL A. (2009): Crystallography Open Database – an open–access collection of crystal structures. *Journal of Applied Crystallography*, **42** 726–729

HAWTHORNE, F.C., OBERTI, R., HARLOW, G.E., MARESCH, V.W., MARTIN, R.F., SCHUMACHER, J.C., & WELCH, M.D. (2012): Nomenclature of the amphibole supergroup, IMA Report. *American Mineralogist* **97** 2031–2048.

JÓZSA, S., SZAKMÁNY, Gy., ORAVECZ, H. & CSENGERI, P. (2001a): Petrography of blueschist stone tools in Hungary. *4th Workshop of the IGCP/UNESCO Project No. 442*, September 24th-28th Udine and Genova (Italy) 24–25.

JÓZSA, S., SZAKMÁNY, GY., ORAVECZ, H. & CSENGERY, P. (2001b): Preliminary petrographic report on blueschists, the material of Neolithic polished stone tools from Hungary. *Slovak Geological Magazine*, **7** 351–354.

KERESKÉNYI E., SZAKMÁNY Gy., FEHÉR B., KASZTOVSZKY Zs., KRISTÁLY F., RÓZSA P. (2016): A Herman Ottó Múzeum neolit kékpala nyersanyagú csiszolt kőeszközeinek előzetes archeometriai eredményei. Itt az idő! 7. Kőzettani és Geokémiai Vándorgyűlés, Debrecen, ISBN 978-963-8321-52-7, 33–36.

KRISTÁLY F. (2014): Rapid non-destructive x-ray diffraction investigation of polished greenstone tools. *Archeometriai Műhely* **XI/4** 223–241

PECHARSKY, V. K. & ZAVALIJ, Y. (2005): *Fundamentals of powder diffraction and structural characterization of materials*. Springer Verlag, Berlin, 371 p.

PÉTERDI, B., SZAKMÁNY, Gy., BENDŐ, Zs., KASZTOVSZKY, Zs., T. BIRÓ, K., GIL, G., HARSÁNYI, I., MILE, V., SZILÁGYI, Sz. (2014): Possible provenances of nephrite artefacts found on Hungarian archaeological sites. *Archeometriai Műhely* **XI/4** 207–222

YOUNG, R.A. ed. (1993): *The Rietveld Method*. Oxford University Press, Oxford, 310 p.

SCHUSTER M. & GÖBEL H. (1995): Parallel beam coupling into channel-cut monochromators using curved graded multilayers. *J. of Applied Physics* **28/A** 270–275.